Fusion Engineering and Design 122 (2017) 341–348

Contents lists available at ScienceDirect

Fusion Engineering and Design

journal homepage: www.elsevier.com/locate/fusengdes

# The DTT device: Divertor solutions for alternative configurations including liquid metals

G. Maddaluno [a], D. Marzullo [b], G. Mazzitelli [a,*], S. Roccella [a], G. Di Gironimo [b], R. Zanino [c]

[a] ENEA-Frascati, Via E. Fermi 45, 00044 Frascati, Italy
[b] CREATE, Univ. Degli Studi di Napoli Federico II – DII, P.le V. Tecchio 80, 80125 Napoli, Italy
[c] NEMO Group, Dipartimento Energia, Politecnico di Torino, Torino, Italy

ARTICLE INFO

*Article history:*
Received 22 July 2016
Received in revised form 23 January 2017
Accepted 14 March 2017
Available online 3 June 2017

*Keywords:*
DTT
Divertor
Liquid metal
Remote handling

ABSTRACT

One of the main objectives of the DTT project is to test many divertor designs and configurations, so that the concept of the machine could change from the initial single null (SN) configuration to other configurations such as the SnowFlake Divertor (SFD). Furthermore the design of Vacuum Vessel, ports and In-Vessel Components should take into account the application and testing of a Liquid Metal Divertor. For this reason the divertor design has been developed having in mind the possibility of easily replacing the divertor itself by remote handling.



## 1. Introduction

The divertor is the most important component of DTT (Divertor Tokamak Test). It will be "conventional" like the standard single null (SN) ITER divertor, adopting the same shape and technology as well as the same tungsten material. It will be an "alternative" divertor to allow for alternative magnetic configurations (SFD- SnowFlake Divertor) that means different geometry of the inner, outer leg and dome but same W material. It will be an "innovative" divertor to test liquid metal as plasma facing components.

In the project, the modularity and the possibility to change the divertor by remote handling in a relatively short time are mandatory.

In this paper a reference divertor for DTT is discussed and possible improvements of the divertor design are investigated.

The DTT preliminary design includes a set of W-shaped solid FAST-like divertor modules [1] displaced toroidally along the vessel (see Fig. 2). This design is compatible with SN and Quasi SnowFlake (QSF) configurations.

They consist of a dome, an inner target plate, an outer target plate (Plasma Facing Unit – PFUs) and a cassette body. The plasma particles strike the targets, so the heat flux is very intense and requires active water-cooling.

In Section 2 we report the preliminary analysis of the SN and QSF divertor in Section 3, while in Section 4 the idea for a liquid metal divertor. Finally, in Section 5, we will discuss the remote handling issue.

## 2. Conventional divertor

DTT will initiate operating with standard SN configuration; however, during this phase several different magnetic divertor configurations will be tested, with the full available additional power. This will allow to compare the performances of the different magnetic configurations and to design a new optimized divertor. The main consequence of this is that the first divertor installed in the machine must be compatible, as much as possible with quite different magnetic configurations.

### 2.1. The initial DTT divertor

The design of the initial DTT divertor is that developed for FAST [1–3]. It is an ITER-like divertor segmented in 72 toroidal sectors or cassettes. Each divertor cassette comprises a cassette body, which supports the plasma facing components (PFCs), an inner (IVT) and outer vertical target (OVT) and a dome. The PFCs are actively cooled by pressurized water. Each cassette body is made of AISI 316L and is designed to withstand the electromagnetic forces, provide shielding for the vacuum vessel and coils, and incorporate water

* Corresponding author.
*E-mail address:* giuseppe.mazzitelli@enea.it (G. Mazzitelli).

http://dx.doi.org/10.1016/j.fusengdes.2017.03.172
0920-3796/

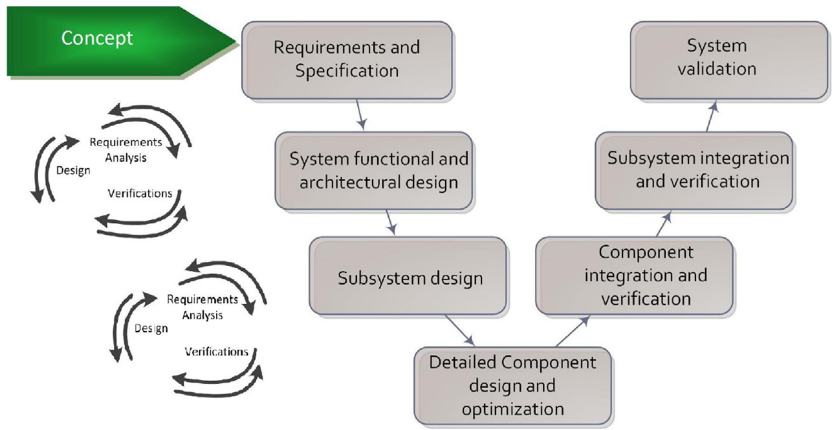


**Fig. 1.** Workflow scheme – V Model.

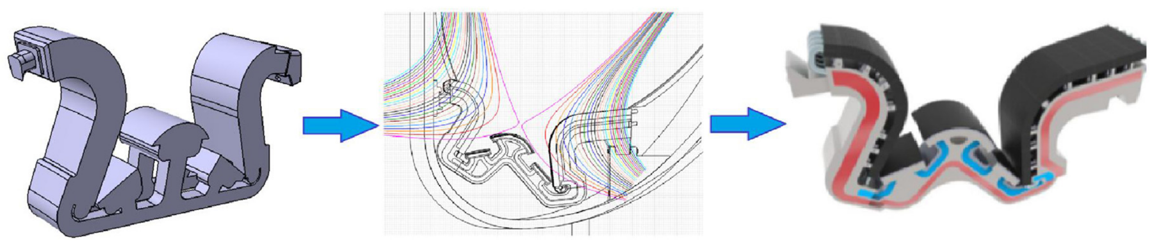

**Fig. 2.** Design of a FAST-like divertor compatible with the SN and the QSF.

**Table 1**
CuCrZr Fatigue Life Estimation [6].

| Max Temp (°C) | Total Strain ($\varepsilon_t$) % | Fatigue number of cycles |
|---|---|---|
| 348 | 0,25 | ~20000 |

channels, which cool the cassette body and act as manifolds for the PFC coolant (Table 1).

The design process of the DTT divertor has been performed according to the Systems engineering Principles (Fig. 1), starting from an ITER-like solution and proceeding iteratively towards optimized solutions.

The conceptual design stage consists of several iteration process starting from requirements analysis, generation of alternative design solutions and their verification against requirements (left side of V-model, Fig. 1). According to this,starting from the first w shape, electromagnetic and structural analyses have been performed iteratively, in order to find the best geometrical configuration DTT divertor geometry, Fig. 2 shows the evolution of the design.

Structural analyses have shown its capability to sustain electromagnetic loads connected with vertical disruption at the plasma current of 6 MA, see Fig. 3 [4].

A preliminary analysis of a conventional divertor cassette has been performed considering the most critical time instant evaluated in the first EM analysis, as shown in Table 2. The structural FE Model has been based on the EM mesh (Fig. 4).

Iterative analyses have been performed, according to the iteration cycles shown in Fig. 1, to find the best configuration in terms of materials and geometrical shape, with respect to the M-type assessment as from the ITER SDC-IC [5]. Fig. 5 shows results in terms of Von Mises stress relative to the optimized geometrical configuration.

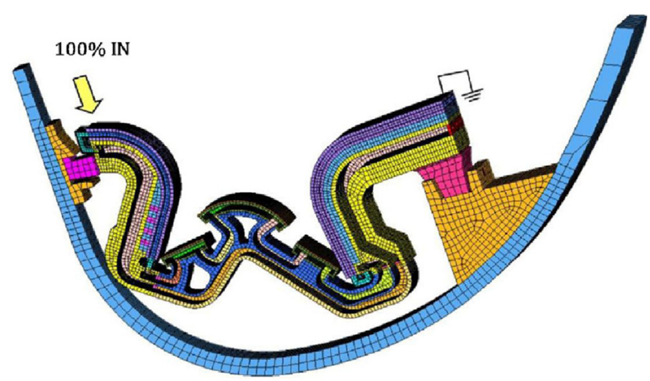


**Fig. 3.** Model used for HC analysis [4].

**Table 2**
Force and Moment from EM analysis.

| Component | Peak Value | Time [ms] |
|---|---|---|
| Fx | 36.28 [kN] | 67.9 |
| Fy | 55.39 [kN] | 74.5 |
| Fz | 119.91[kN] | 67.9 |
| Mx | 4.01 [kNm] | 67.8 |
| My | −9.29 [kNm] | 75 |
| Mz | 3.52 [kNm] | 67.8 |

Basing on the analyses results, a final geometrical configuration for the DTT conventional divertor cassette has been designed, as shown in Fig. 6.

### 2.2. DTT divertor PFUs

The IVT consists of 4 PFUs, while the OVT of 6. The PFUs use the same concept of the ITER units: the cooling tubes in

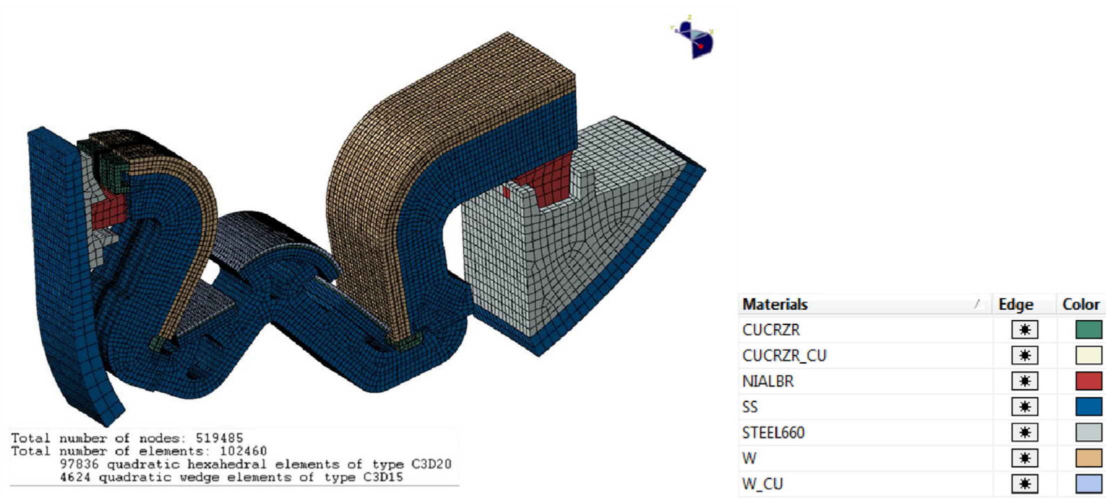


**Fig. 4.** Structural FE Model.

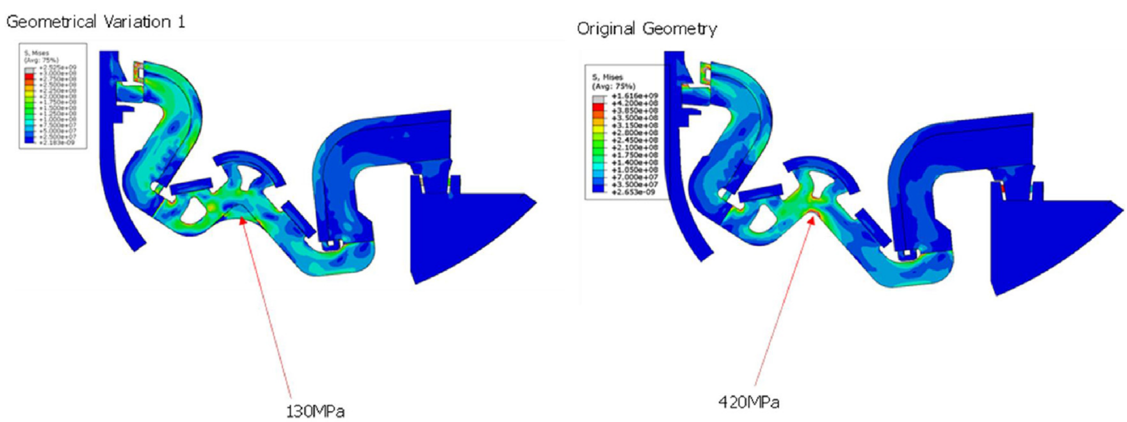


**Fig. 5.** DDT divertor analysis. Von Mises stress.

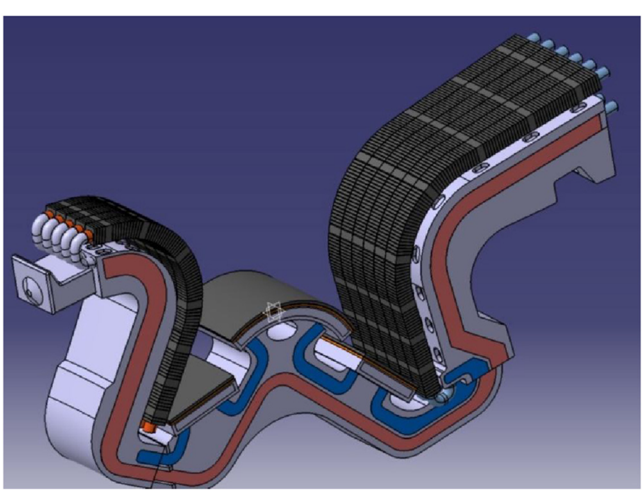

**Fig. 6.** Final divertor concept design as result of remote handling and structural analyses.

CuCrZr are coated with a tungsten monoblock armour and welded together through an OFHC Cu interlayer which reduces the thermal stresses between the two materials ensuring the appropriate thermal exchange. The ITER configuration consist of a cooling tube of inner diameter 12 mm and thickness 1.5 mm, interlayer 1 mm and tungsten monoblock thickness in axial direction 12 mm. This configuration is currently the most robust and is qualified to withstand 1000 cycles to 10 MW/m$^2$ and 300 cycles to 20 MW/m$^2$.

In the frame of the DEMO divertor activities the production of PFU mock-ups, with optimized geometry monoblocks and with 4 mm thickness to reduce the stresses generated by the heat loads on the cooling pipe CuCrZr [6], is ongoing. The option with copper pipes was discarded for DEMO due to the degradation of the mechanical properties under neutronic radiation. However, it was noticed that, if the copper pipes are kept in a specific temperature range (200–400 °C), the degradation of their mechanical properties remains within acceptable limits. Hence, it has been decided to increase the temperature of the cooling water up to 200 °C and to not discard the safest option from the technological point of view. Mock-ups with other options, with respect to the CuCrZr one, will be manufactured and tested. Results of thermal fatigue tests will give additional indications on the maximum admissible loads with the present technology and give hints for possible alternatives.

In the PFUs of the first DTT divertor the pipe size and the interlayer thickness have been taken equal to the ITER ones; on the other hand, the adopted monoblock thickness of 4 mm is the one envisaged for DEMO. Thicker monoblocks (12 mm) have been maintained only in correspondence of the junction between the divertor and the cassette body. The necessity to cover a toroidal suface implies the use of different thickness of the monoblocks in toroidal direction at different positions and, due to the small dimen-

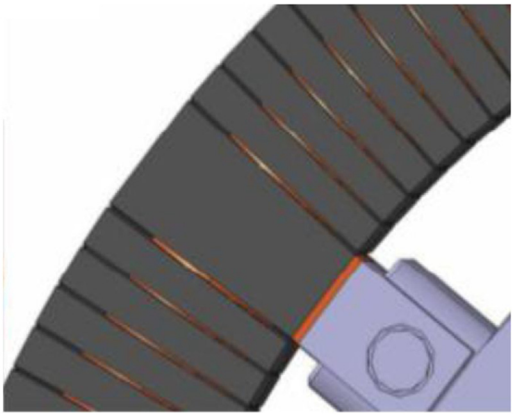

**Fig. 7.** V-Shaped Tiles for the curved Target [1].

sions, to follow the curvature of the pipe non parallel monoblocks will be used (see Fig. 7).

In the region of the separatrix strike points of the inner and outer targets, inclined at 30° and 20° respectively with respect to the separatrix itself, the PFUs have been optimized to maximize the radial local losses. On the top, the targets are connected to a flat part, particularly evident in the OVT, by a blended part. Both of these parts have been designed to allow large flexibility of the magnetic configuration (Fig. 2).

### 2.3. PFUs thermo-mechanical analysis

For the SN magnetic configuration, a calculation of the PFU fatigue life with a maximum heat load of about 20 MW/m2 was made in [7]. In the model, pressurized water @4 MPa and 140 °C inlet temperature flows in the PFUs pipe at 20 m/s. A twist tape is included in the straight part of the PFU. The thermal load decreases exponentially in the axial direction. The design evaluation of the divertor is performed using the ultimate tensile strength for W and the Low Cycle Fatigue Curves (LCFC) for CuCrZr and Cu-OFHC.

The thermal analysis has been carried out with a CFD code. The Shear Stress Transport Turbulence model was used and the sub-boiling regime was not considered because the max temperature reached by the water of 180 °C is under the boiling temperature at the reference pressure. The temperature at the plasma facing W surface is shown in Fig. 8; the maximum at the strike point is 1641 °C.

The results of the mechanical analysis (Fig. 9) show a high circumferential stress in the W monoblocks, approaching the ultimate tensile strength (1050 MPa) at the temperatures of interest.

The results obtained show a satisfying fatigue life (I) but the high circumferential stress in the Tungsten suggests the possibility of cracks opening in the direction parallel to the pipe axis, similar to those observed in mock-ups after thermal fatigue testing up to 20 MW/m$^2$ [7].

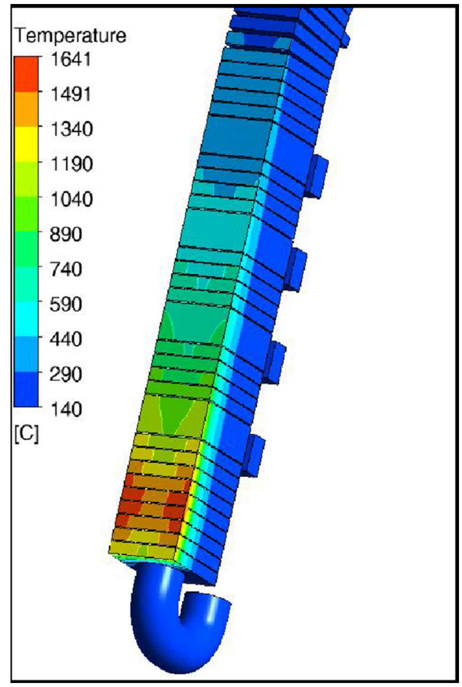


**Fig. 8.** Temperature (°C) distribution on the OVT for the SN configuration [7].

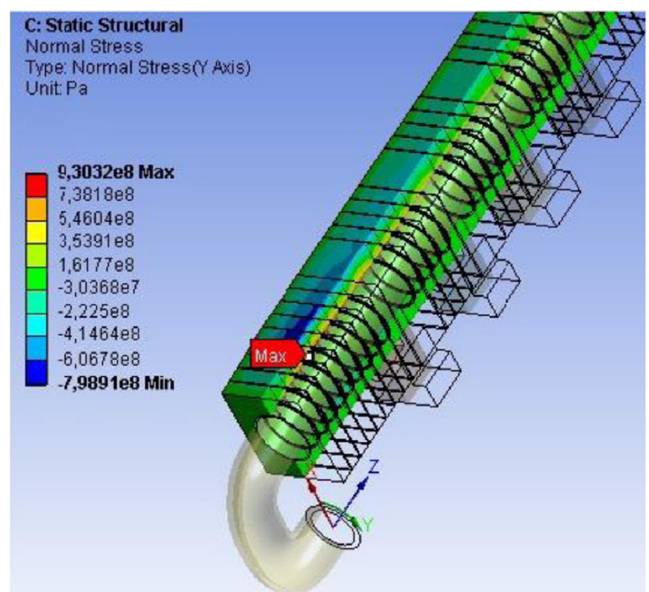


**Fig. 9.** Circumferential Stress (Pa) on the monoblock [7 4].

## 3. QSF versus SN heat loads for the reference standard scenario

The SN divertor concept seeks to flare the flux surfaces near the divertor targets. The flaring is obtained by decreasing the poloidal magnetic field at the target. The lower field at the target leads to an increase of the connection length, L||, which is expected to decrease the plasma temperature at the target and lead to detachment at lower densities or higher exhaust power. The snowflake divertor (SFD) also provides an increased connection length and divertor volume. However, the corresponding decrease of the poloidal field is obtained by introducing a second order null point. This splits the separatrix around the null into six legs with two enclosing the confined plasma and four divertor legs. Since the exact SFD is only a point in the operational plane any real configuration is characterised by two nearby first order null-points (x-points). The SF configurations are characterised by a particularly large flux expansion in the null point region. As the location of the secondary x-point approaches the target, the configuration has a transition toward an SN. Such configurations with two x-points in the divertor are also referred to as quasi-snowflake (QSF) configurations.

In the SN reference scenario, a thermal load of $q_0 = 20\,MW/m^2$ on the vertical targets is possible only with high radiation power in the SOL by impurity injection [8]. Such impurities are not needed in the QSF configuration The peak loads seem sustainable without

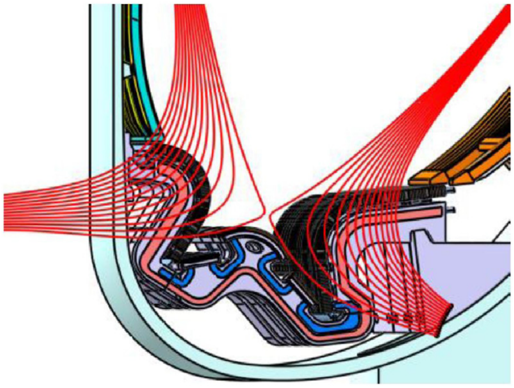

**Fig. 10.** QSF flux lines.

requiring particular care in the tilt of the target, which needs only a sufficient poloidal length (Fig. 10).

Furthermore the plasma electron temperature at the strike point is well below the W sputtering threshold, therefore all risks connected to the influx of high Z impurities in the core from the target should be strongly alleviated. The effect is mainly driven by the great flux expansion that is realized in the outer target. Instead, on the inner target the expansion is at present significantly lower, but here the uneven share of the power load between the two targets consistently reduces the problem.

An additional thermo-hydraulic analysis has been made on the OVT of the initial DTT divertor to evaluate the possibility to operate with QSF configuration without replacing the Divertor. The thermal load along the target surface was estimated in the extreme case of 30 MW of power in the SOL. The SOL radiation losses were neglected while the power asymmetry of the divertor legs was considered and the power was split between inner and outer vertical target in ratio of 1:2. Moreover the possibility to move vertically the X-point inside a range of ±40 mm was considered and the analysis was made at the most critical condition of 40 mm X-point upward shift. In the QSF analysis the bigger expansion factor (F) caused the heat flux to load the upper curved part of the PFU impinging a surface larger than SN. To estimate the incident heat flux, the expansion coefficient, F, and the incident angle for the field lines in the poloidal cross section, β, were evaluated as a function of the abscissa along the pipe axis, s. The following law was applied:

$$q(s) = q_0 e^{\frac{-s \sin\beta(s)}{\lambda F(s)}}$$

where F(s) and β(s) were 5th order appropriate polynomials and $q_0 = 14\,\mathrm{MW/m^2}$.

The temperature distribution, applying the same hydraulic parameters (140 °C, 4 MPa e 2.2 kg/s), as for the SN configuration, is reported in Fig. 11 with a maximum value of 1126 °C on the W.

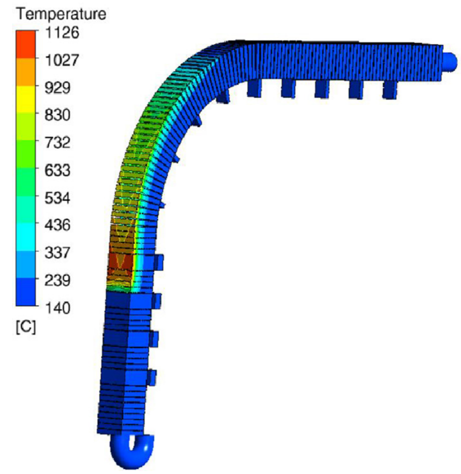


**Fig. 11.** Temperature (°C) distribution on the PFU for the QSF configuration [7 4].

## 4. Liquid metal divertor

Liquid metal PFCs show higher heat exhaust capability than solid targets and may relax some constraints on the power and particle exhaust and, thereby, increase the lifetime of the PFCs.

Liquid metals are attractive because of their high boiling temperature and their high heat conductivity. A range of liquid metals is currently considered with lithium (Li) and tin (Sn) being likely candidates for low *Z* and high *Z* metals, respectively.

The least complex and hence most promising liquid metal are based solutions on a stationary liquid which is confined in a porous system [9,10]. While these capillary porous system (CPS) based solution have only a limited potential for enhanced heat removal [11], they can increase the lifetime of the divertor targets by in situ replenishment of eroded material, avoiding any net-material loss, and repair of the surface, preserving its physical and chemical properties. They also avoid primary lattice defect production possibly leading to defect accumulation, which is responsible for surface modifications, swelling and general material degradation (cracking). The in situ replenishment also increases the tolerance to uncontrolled or partially controlled transients by allowing temporary evaporation, thereby, transferring plasma energy into latent heat and possibly creating a high density neutral cushion in front of the target (so-called vapour shielding) while avoiding net erosion and surface modifications [11].

In a CPS the liquid is confined inside a porous structure, such as a mesh, felt or porous solid, which is wetted by the liquid metal. Wetting is an important condition, which can be provided by adhesive forces resulting from intermolecular forces. The adhesive forces act against surface tension forces, which aim to form a sphere to minimise surface energy. Wetting has to be guaranteed under all conditions.

The stationary heat removal of a CPS system is based on the heat transport through the target to the cooling medium. The target consists of the liquid with its confining system and the underlying, actively cooled structure. The heat transport, $q_{\mathrm{target}}$, through the structure predominantly happens by conduction. In a one dimensional system the heat flux,

$$q_{\mathrm{target}} = \frac{T_{\mathrm{surf}-} T_{\mathrm{coolant}}}{\Sigma_k d_k/\lambda_k}, \tag{2.4.3}$$

is determined by the difference between the surface temperature, $T_{\mathrm{surf}}$, and the coolant temperature, $T_{\mathrm{coolant}}$, and the ratio between thickness, $d_k$, and the effective heat conductivity, $\lambda_k$, of each component (e.g. mesh with liquid, substrate, coolant pipe) between the surface and the coolant. The maximum allowable surface temperature is determined by the maximum evaporation rate that is acceptable for plasma compatibility and other boundary conditions. The allowable evaporation rate depends on the screening of evaporated species inside the divertor and the core plasma compatibility [12]. Other boundary conditions can for example arise from tritium retention. The core plasma compatibility will likely set the limit for high *Z* liquids, whereas fuel dilution and tritium retention are expected to be limiting for the low Z metal Li. It is, however, possible that other components of the target (e.g. CuCrZr cooling pipes[13]) impose more severe constraints on the temperature range, and hence on the heat removal capability of the target.

The effective evaporation rate, which greatly determines the performance of the liquid metal target concept, is enhanced over

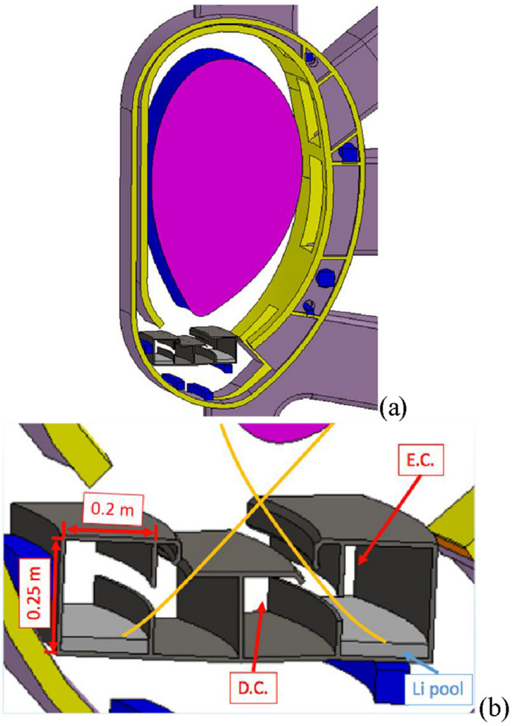


**Fig. 12.** (a) DTT main plasma chamber with the divertor highlighted and (b) preliminary sketch of the LM divertor.

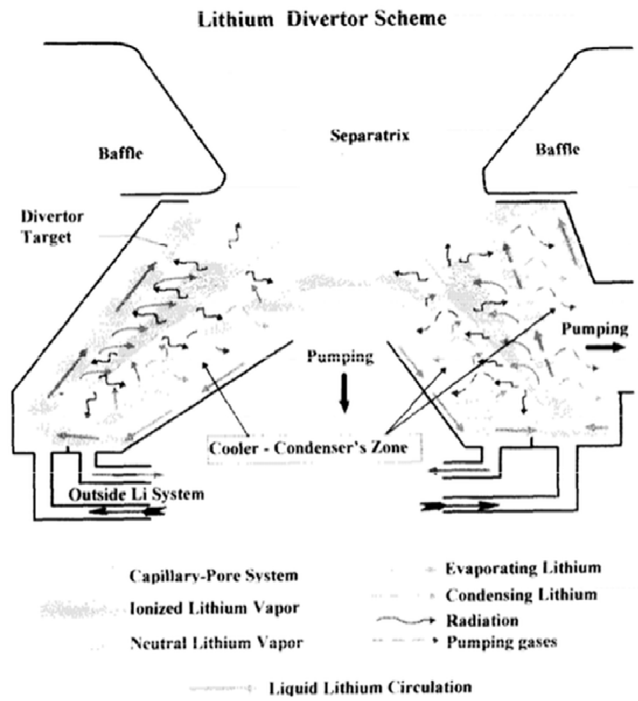


**Fig. 13.** The scheme of a possible liquid metal divertor as proposed in [9].

the thermal evaporation rate under plasma impact. Erosion through classical physical sputtering is reasonably well described by the binary collision model. Recently, an "abnormal" erosion mechanism is discussed acting at high temperatures, which can be also important for the use of liquids [14]. Similarly, possible chemical erosion effects may play a role [15,16].The effective target erosion, which has to be replenished through the CPS, is greatly reduced by prompt ionisation and subsequent local redeposition of the eroded species, analogous to the reduced net-erosion rate of solid targets [17].

A preliminary model of a possible LM divertor has been recently developed at PoliTo [18] for the proposed DTT facility. The initial assumption for the choice of LM was Li, but the same model could also be used to study parametrically the effects of other choices, e.g. Sn, provided the needed input atomic data are or become available.

The proposed approach includes in a first step a Li pool, see Fig. 12, as target for the plasma heat load, which is the simplest option among those proposed in [19]. The pool is contained in the so called evaporation chamber (EC), which is connected through a nozzle to the adjacent differential chamber (DC) – the first in a series of such chambers in the box divertor concept [20] – which in turn is connected, again through a nozzle, to the main plasma chamber (MC). Both the EC and the DC have actively cooled walls.

A simplified 0D (thermodynamic) model for the LM divertor was proposed, where the following main phenomena are included:

- the evaporation of the Li from the target, due to the plasma load;
- the Li vapour flow between the chambers (in the ideal gas assumption), and its interaction with the incoming plasma, following the simplified treatment proposed in [ref. goldston];
- the re-condensation of the LM on the chambers' walls, including the evaluation of the heat flux onto them, to be eventually exhausted by the coolant (presently modelled with a given heat transfer coefficient HTC and a fixed temperature heat sink);

Code results show that the expected temperature of the Li system are of the order of 900–1000 K, that could be reasonable and gives an important information on the first wall material that could be compatible with hot Li.

To overcome some possibly geometrical incompatibilities with the closed-box divertor approach we are also taking into account the approach presented in ref [9], see Fig. 13.

At the beginning a prototype module will be designed, manufactured and installed on the machine to test the proposed solution. The module should be compatible with the other tungsten modules, i.e. it should be shaped taking into account the magnetic geometry and particle and heat fluxes avoiding to create zones with intolerable heat loads.

## 5. Divertor remote handling

The expected neutron rate in DTT varies from a minimum of $0.3 \times 10^{17}$ ns$^{-1}$ for AT scenarios to a maximum of $1.3 \times 10^{17}$ ns$^{-1}$ for the H-mode extreme scenario. The short/medium term activation is not negligible, making remote handling (RH) mandatory for maintenance and replacement of in-vessel components. To accomplish these operations DTT will be equipped with a Remote Maintenance System; this includes the Remote Handling equipment set and a "Shielded and restricted area" required for the execution of repair operations and for temporary storage of the operational and decommissioning radwaste. Both need to work in a cooperative way, with the aim of minimizing the machine shutdown periods and to maximize the machine availability.

The flexibility required to DTT in terms of divertor configurations testing, makes the DTT divertor RH system issues quite different from the others existing tokamak. It is required to provide an easy handle of different type of divertor cassettes, characterized by different magnetic configurations or different operating principles. Since one of the main DTT target is the study of the power exhaust, the divertor choice cannot be limited on a SN and/or a SF, but the machine must have the possibility to test also other possible options, like, for instance, a liquid metal divertor [21,22]. For this reason the design of the divertor remote handling system has to be

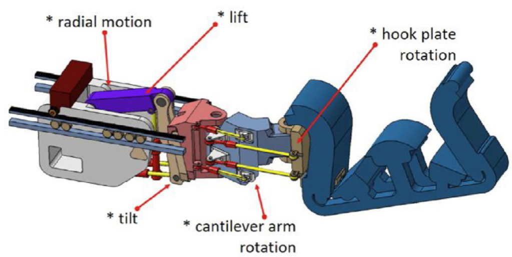


**Fig. 14.** Schematic view of the Divertor remote handling system.

implemented having in mind the possibility of easily replace different divertor cassettes to study alternative magnetic configurations and power exhaust system [23,24]. At the same time, the DTT RH equipment is required to be available, robust, reliable and retrievable and the divertor configurations are required to be designed to ease their maintenance.

At present, an ITER-like remote handling system for cassette transportation has been considered [25–27]. It consists of a Cassette Multifunctional Mover (CMM) equipped with an end effector composed by a lifting arm, a tilting plate, a cantilever arm and a hook-plate (Fig. 14). The basic idea for the DTT divertor RH system is to design an end effector as much as possible independent from the divertor configurations, in order to have a flexible system able to deal with the transport of different alternative cassettes. Furthermore, the possibility to change the cassette end effector between two different plasma configurations is considered as alternative option.

The divertor configuration must account for an easy maintenance operation via the lower ports. Fig. 15 shows a first possible motion sequence of the cassette during the maintenance operation, compatible with DTT VV design [28]. To allow such maintenance technique the internal coil attached to the divertor should be modular and allow an easy dismounting.

The CMM is also equipped with an ITER-like robotic arm able to operate by means of RH tools on cassette fixation system, cooling pipes connection/disconnection, dismantling of internal coils interfering with the cassette removal/installation (Fig. 15) [29]. Unlike SN and SF, the liquid metal divertor requires additional feeding pipes for liquid lithium. This will affect maintenance time and RH tools design, since the robotic arm has to be able to operate the connection/disconnection of such different kind of pipes.

In addition to the capability of complete substitution of divertor cassettes, the non-negligible possibility of substitution of several parts of the divertor modules must be considered. This concerns especially the plasma facing components, due to the short and medium-term activation of modules. Furthermore, this capability will allow testing different plate geometries or materials able to

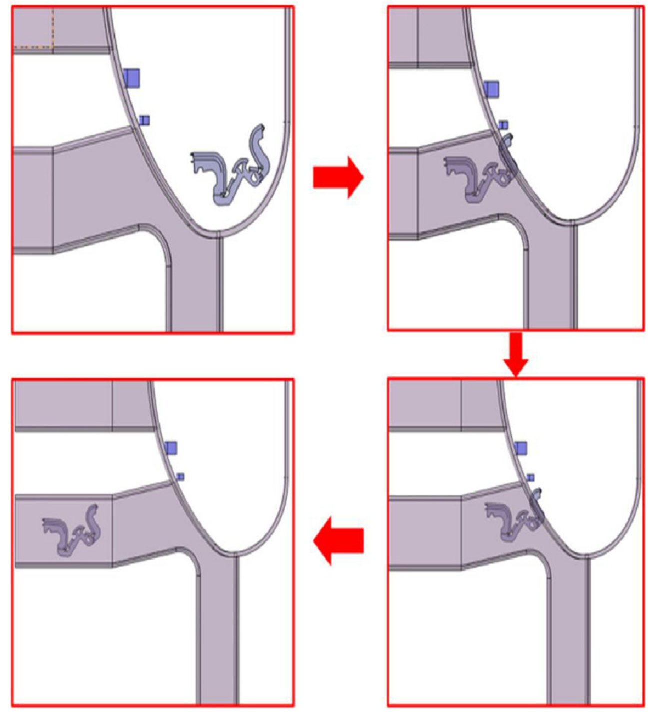

**Fig. 15.** Motion sequence of the divertor cassette.

improve the plasma performance. Such operations of parts substitution will be performed in a “shielded and restricted area”, and this is the main reason why the realization of a Remote Handling Facility plays a crucial role in operations of the whole DTT tokamak.

The guideline of the future work foresees several steps oriented to provide a series of alternative or innovative proposals for DTT divertor remote maintenance, starting from an ITER-like solution and then proceeding through an interactive design review (Fig. 16). According to a systems engineering approach the whole process starts with the identification of RH requirements and several design issues [30].

Based on these requirements, several concepts are proposed and evaluated iteratively through requirements analysis and verification. The concepts are designed in CAD software, performing simulations and analyses that can help comparing the alternatives. A set of criteria is thus selected, on which the comparison of concepts will be performed, following the AHP methodology [2,31]. The final evaluation session is carried out in virtual reality environment, involving several experts in the judgment, during participative design review sessions.

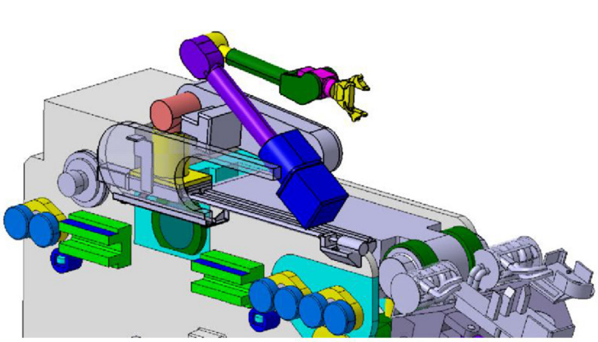

a

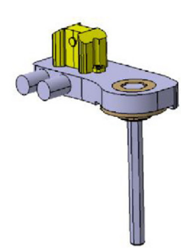

b

**Fig. 16.** a) ITER robotic manipulator; b) ITER RH tool for cassette fixation.

## 6. Conclusions

Considering the relevant problems about the interaction between plasma and surrounding materials, the optimization of the divertor geometry represents one of the key points in the whole DTT project. Such an aim can be achieved, initially, by studying the plasma boundaries, including all the real geometry conditions, from the physics point of view and without a deep attention to engineering constraints, which provides an optimized “conceptual” geometry. Then, in a second step, such a solution needs to be tackled with all the mechanical design problems, including the remote maintenance tools. Starting from the work done for the FAST project, the conventional divertor for DTT has been discussed as well as its adaptability to advanced magnetic configurations (e.g. SF). Preliminary ideas about a liquid metal divertor have been presented. In DTT the substitution in a safe and fast way of the divertor is important to guarantee the exploitation flexibility of the machine, so that since the beginning special attention has been put on the divertor remote handling facility

## Acknowledgements

This work has been carried out within the framework of EUROfusion (European Consortium for the Development of Fusion Energy) and has received funding from the Euratom research and training programme 2014-2018 under Grant Agreement No. 633053. The views and opinions expressed herein do not necessarily reflect those of the European Commission.

## References

[1] G. Di Gironimo, et al., Innovative design for FAST divertor compatible with remote handling, electromagnetic and mechanical analyses, Fusion Eng. Des. 98–99 (2015) 1465–1469.
[2] G. Di Gironimo, et al., Improving concept design of divertor support system for FAST tokamak using TRIZ theory and AHP approach, Fusion Eng. Des. 88 (2013) 3014–3020.
[3] G. Di Gironimo, et al., Concept design of divertor remote handling system for the FAST machine, Fusion Eng. Des. 88 (2013) 2052–2056.
[4] I. Pagani, et al., Preliminary electromagnetic design for divertor of FAST, Fusion Eng. Des. 88 (2013) 2173–2176.
[5] Standard Design Code-In-vesell Components, ITER_D_222RHC.
[6] F. Crescenzi, et al., Design study of ITER-like divertor target for DEMO, Fusion Eng. Des. 98–99 (2015) 1263–1266.
[7] F. Crescenzi, et al., Vessel and in-vessel components design upgrade of the FAST machine, Fusion Eng. Des. 88 (2013) 2048–2051.
[8] V. Pericoli Ridolfini, et al., Comparative study of a conventional and snowflake divertor for the FAST (fusion advanced studies torus) tokamak, J. Nucl. Mater. 438 (2013) S414–S417.
[9] L.G. Golubchikov, et al., Development of a liquid-metal fusion reactor divertor with a capillary-pore system, J. Nucl. Mater. 233–237 (233) (1996) 667––.
[10] V.A. Evtikhin, Calculation and experimental investigation of fusion reactor divertor plate and first wall protection by capillary-pore systems with lithium, J. Nucl. Mater. 271–272 (271) (1999) 396–400.
[11] J.W. Coenen, et al., Liquid metals as alternative solution for the power exhaust of future fusion devices: status and perspective, Phys. Scr. T159 (2014).
[12] D. Post, et al., Calculations of energy losses due to atomic processes in tokamaks with applications to the International Thermonuclear Experimental Reactor divertor, Phys. Plasmas 2 (1995) 2328–2336.
[13] J.-H. You, DSivertor PFC Concepts Considered in the DEMO Divertor Project, EFPW, Split, Croatia, 2014, Dec 1–3.
[14] T. Abrams, et al., Modeling the reduction of gross lithium erosion observed under high-flux deuterium bombardment, J. Nucl. Mater. 463 (2015) 1169–1172.
[15] M.D. Coventry, et al., Temperature dependence of liquid Sn sputtering by low-energy $He^+$ and $D^+$ bombardment, J. Nucl. Mater. 335 (2004) 115–120.
[16] R.P. Doerner, et al., Measurements of erosion mechanisms from solid and liquid materials in PISCES-B, J. Nucl. Mater. 290–293 (2001) 166–172.
[17] R. Ding, et al., Modelling of lithium erosion and transport in FTU lithium experiments, J. Nucl. Mater. 438 (2013) S690.
[18] G.F. Nallo et al. Modeling the lithium loop in a liquid metal divertor for DTT, submitted to Fusion Engineering and Design (Presented at IADIS-1 Workshop Oct. 14th and 15th, 2016. Kyoto, Japan.).
[19] Y. Nagayama, Liquid lithium divertor system for fusion reactor, Fusion Eng. Des. 84 (2009) 1380–1383.
[20] R.J. Goldston, et al., The lithium vapor box divertor, Phys. Scr. (2016) 014017, http://dx.doi.org/10.1088/0031-8949/t167/1/014017.
[21] V. Pericoli-Ridolfini, et al., Edge properties with the liquid lithium limiter in FTU—experiment and transport modelling, Plasma Phys. Controlled Fusion 49 (7) (2007) S123.
[22] G. Mazzitelli, et al., FTU results with a liquid lithium limiter, Nucl. Fusion 51 (2011) 073006 (7).
[23] G. Di Gironimo, et al., An interactive design approach for nuclear fusion purposes: remote handling system for FAST divertor, Int. J. Interact. Des. Manuf. 8 (1) (2014) 55–65, http://dx.doi.org/10.1007/s12008-013-0194-z, Publisher Springer Paris.
[24] G. Di Gironimo, et al., Concept design of divertor remote handling system for the FAST machine, Fusion Eng. Des. 88 (2013) 2052–2056, http://dx.doi.org/10.1016/j.fusengdes.2013.02.035, ISSN: 09203796, Elsevier. WOS:000326903200131.
[25] J. Palmer, et al., The design and development of divertor remote handling equipment for ITER, Fusion Eng. Des. 82 (15) (2007) 1977–1982.
[26] F. Crisanti, et al., FAST: A European ITER satellite experiment in the view of DEMO, Fusion Eng. Des. 86 (October (6–8)) (2011) 497–503.
[27] A. Cucchiaro, et al., Engineering evolution of the FAST machine, Fusion Eng. Des. 86 (October (6–8)) (2011) 703–707.
[28] G. Di Gironimo, et al., The DTT device: first wall, vessel and cryostat structures, Fusion Eng. Des. (2016) (in press).
[29] P. Nieminen, et al., Water hydraulic manipulator for fail safe and fault tolerant remote handling operations at ITER, Fusion Eng. Des. 84 (7) (2009) 1420–1424.
[30] G. Di Gironimo, et al., Iterative and participative axiomatic design process in complex mechanical assemblies: case study on fusion engineering, Int. J. Interact. Des. Manuf. (IJIDeM 9 (4) (2015) 325–338.
[31] D. Marzullo, et al., Design progress of the DEMO divertor locking system according to IPADeP methodology, Procedia CIRP 34 (2015) 56–63.